Progress In Electromagnetics Research C, Vol. 76, 43–54, 2017

Unbalanced-to-Balanced Power Divider With Arbitrary Power Division

Amar N. Yadav* **and Ratnajit Bhattacharjee**

Abstract—In this paper, Gysel type Unbalanced-to-Balanced (UTB) Power Divider (PD) with arbitrary power division is proposed. UTB PD is a five-port device, and a standard scattering matrix for a five-port PD with arbitrary power division is derived. Design equations are obtained analytically. Using design equations, a UTB PD is designed at 2 GHz for power division ratio of 1 : 2, and simulation is carried out using HFSS. A prototype is fabricated, and measurement is performed to verify the simulation results of PD. Measured results are in good agreement with the simulated ones. The proposed PD shows in-phase characteristic within $\pm 5^{\circ}$. Measurement results show that isolation between two output ports is greater than 20 dB. Greater than 20 dB common-mode suppression from input port to output balanced ports is achieved. Differential-mode power is divided in power division ratio of 1 : 2 from unbalanced port to balanced ports. Measured fractional bandwidth of the proposed PD is 21%.

1. INTRODUCTION

In modern communication systems, differential transceiver is used to eliminate common-mode noise. Several differential circuits are used to design differential transceiver such as differential power divider, differential filter and differential amplifier. Among the various differential circuits, differential PD is used to divide/combine power [1–3]. In general, there are two types of PDs reported in the literature. The first one is Wilkinson PD [4], and the second one is Gysel PD [5]. Size of a Gysel PD is much larger than a Wilkinson PD. In a Wilkinson PD, isolation resistor is connected between the output arms. Therefore, this configuration cannot be used for high power applications. In a Gysel PD, the isolation resistor is connected with the ground which allow heat to be transferred to the ground plane effectively. Therefore, a Gysel PD configuration can be used for high power applications. In past several years, single-ended PDs are extensively investigated. Some of the reported Gysel type single-ended PDs are available in [6–12].

Of late, there is lot of interest in balanced-to-unbalanced (BTU) and unbalanced-to-balanced (UTB) PDs because they have the characteristic of balanced circuit and can be easily connected to single-ended devices. Block diagrams of BTU and UTB PD are shown in Fig. 1(a) and Fig. 1(b), respectively. In BTU PD, input port is balanced while the output ports are single-ended. As shown in Fig. 1(a), input balanced port is port A, and output single-ended ports are ports 1 & 3. In a UTB PD, input port, shown as port 1, is single-ended, and output ports, shown as ports A & B, are balanced.

Various types of BTU PDs are reported in the literature such as [13–16]. BTU PDs for equal power division are reported in [13–15], and that for arbitrary power division is reported in [16]. UTB equal PDs are reported in [17–20]. In [17], UTB equal PD is designed using Mrachand balun, but no isolation element is present in the design. Therefore, two balanced ports of UTB PD reported in [17] are not isolated. In [18] and Section 2 of [19], similar structures of Wilkinson type UTB equal PD are reported. Performance of a PD reported in [19] is better than the PD reported in [18]. These two PDs,

Received 15 June 2017, Accepted 8 July 2017, Scheduled 24 July 2017
* Corresponding author: Amar Nath Yadav (amariitr@yahoo.co.in).
The authors are with the Indian Institute of Technology Guwahati, India.

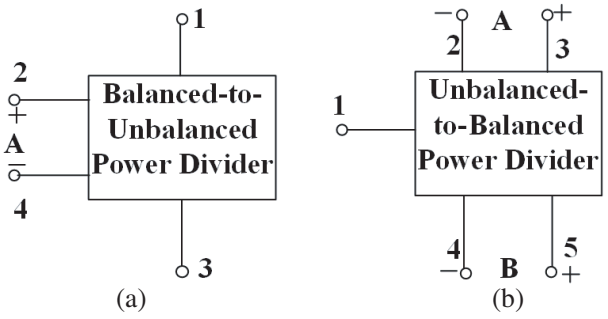

Figure 1. (a) Block diagram of BTU PD. (b) Block diagram of UTB PD.

reported in [18] and [19], are of Wilkinson type. Therefore, these PD configurations cannot be used for high power applications. In [20], another Wilkinson type compact UTB equal PD using coupled lines is reported. A power divider with arbitrary power division gives flexibility to dividing power in specific ratio. Therefore, arbitrary PDs are more versatile than equal PDs. To the best of the authors' knowledge, UTB PD with arbitrary power division is not reported in the literature.

In this paper, a UTB PD for arbitrary power division is presented. Design equations are derived analytically to divide power from input single-ended port to output balanced ports in a specific power division ratio. The proposed PD is of Gysel type; therefore, this configuration can be used for high power applications as well.

2. ANALYSIS OF PROPOSED UTB PD

2.1. Circuit Diagram

Circuit diagram of the proposed UTB PD is shown in Fig. 2. As shown in Fig. 2, port 1 is the input unbalanced port, and port A (combination of ports 2 & 3) and port B (combination of ports 4 & 5) are the balanced output ports of proposed PD. In the circuit diagram, there are two transmission lines of characteristic impedances Z_1 and Z_2, having electrical lengths $\pi/2$ and $3\pi/2$, respectively. There are two pairs of transmission lines of characteristic impedances Z_3 and Z_4. The electrical lengths of these lines are the same and equal to $\pi/2$. There is one pair of transmission lines of electrical length π having characteristic impedances Z_A and Z_B. As shown in Fig. 2, two isolation resistors (both marked as R) provide isolation between ports A & B and are connected with the ground.

Since transmission line parameters are different at different frequencies and constitute a matrix,

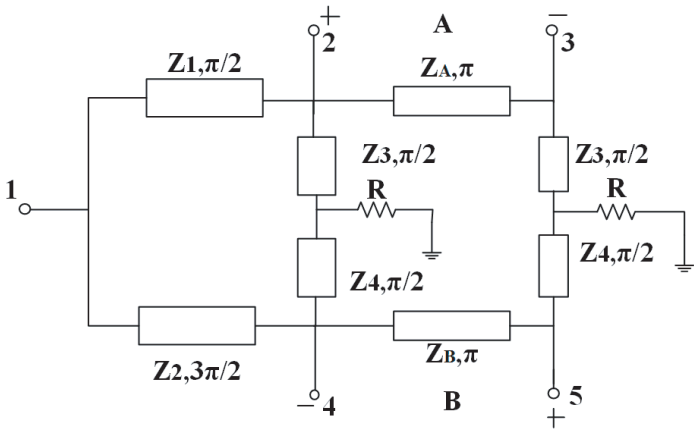

Figure 2. Circuit diagram of proposed UTB PD.

the design can start with a set of frequencies with a certain relation between those, or it can be started with a single frequency approach. In this paper, single frequency approach is adapted. All transmission line lengths are specified at the center frequency. At the input end of the circuit shown in Fig. 2, two transmission lines of lengths $\pi/2$ and $3\pi/2$ are used. The phase difference of 180° between these two transmission lines is required to maintain the phase characteristic of output signals.

First, a standard scattering matrix for a five-port UTB PD for arbitrary power division is derived. The circuit of the proposed PD is not symmetrical. Therefore, conventional even- and odd-mode analysis can not be used. A different analysis technique is presented in [6, 7] to analyze a non-symmetrical single-ended PD. To analyze the proposed unsymmetrical UTB PD, the method described in [6, 7] is adopted. The analysis of the proposed PD is done in two parts. First part is the analysis of power transmission from unbalanced port 1 to balanced ports A and B under ideal conditions, and second part is isolation analysis.

2.2. Formulation of Standard Scattering Matrix

The proposed UTB PD is characterized by its mixed-mode scattering matrix. The mixed-mode scattering matrix of PD is given in Eq. (1).

$$[S^m] = \begin{bmatrix} S_{ss11} & S_{sd1A} & S_{sd1B} & S_{sc1A} & S_{sc1B} \\ S_{dsA1} & S_{ddAA} & S_{ddAB} & S_{dcAA} & S_{dcAB} \\ S_{dsB1} & S_{ddBA} & S_{ddBB} & S_{dcBA} & S_{dcBB} \\ S_{csA1} & S_{cdAA} & S_{cdAB} & S_{ccAA} & S_{ccAB} \\ S_{csB1} & S_{cdBA} & S_{cdBB} & S_{ccBA} & S_{ccBB} \end{bmatrix} \tag{1}$$

where S_{ddAA}, S_{ccAA} and S_{dcAA} are differential reflection coefficient, common-mode reflection and differential to common-mode conversion coefficient for balanced port A, respectively. S_{ddBB}, S_{ccBB} and S_{dcBB} are differential reflection coefficient, common-mode reflection and differential to common-mode conversion coefficient for balanced port B, respectively. S_{sd1A} and S_{sd1B} represent differential-mode transmission coefficients from port 1 to balanced ports A and B. S_{sc1A} and S_{sc1B} denote common-mode suppression (CMS) from unbalanced to balanced ports. S_{ccAB} and S_{ccBA} denote common-mode isolation between two balanced ports. S_{ss11} and S_{ddAB} are reflection coefficient of unbalanced port and isolation between balanced ports, respectively.

For an ideal UTB PD with arbitrary power division, the requirements in terms of mixed-mode parameters are similar to the reported UTB PDs in [18, 20]. The only differences are in terms of power division from unbalanced port to balanced ports. UTB PDs which are reported in [18, 20] are for equal power division. For arbitrary power division, power should be divided from unbalanced port 1 to balanced ports A and B in a specific ratio.

$$|S_{dsA1}| = |S_{sd1A}| = \alpha \tag{2}$$

$$|S_{dsB1}| = |S_{sd1B}| = \sqrt{1-\alpha^2} \tag{3}$$

where, α $(0 < \alpha < 1)$ is the transmission coefficient from port 1 to port A.

Based on the requirements for UTB PD given in [18, 20] and Eqs. (2)–(3), mixed-mode scattering matrix is derived and given in Eq. (4).

$$[S^m] = \begin{bmatrix} 0 & \alpha e^{j\theta_1} & \sqrt{1-\alpha^2}e^{j\theta_2} & 0 & 0 \\ \alpha e^{j\theta_1} & 0 & 0 & 0 & 0 \\ \sqrt{1-\alpha^2}e^{j\theta_2} & 0 & 0 & 0 & 0 \\ 0 & 0 & 0 & e^{j\theta_3} & 0 \\ 0 & 0 & 0 & 0 & e^{j\theta_4} \end{bmatrix} \tag{4}$$

where, $\theta_1, \theta_2, \theta_3, \theta_4$ represent the angles of different mixed-mode scattering parameters. For the proposed PD, $\theta_1 = \theta_2 = -\pi/2$ and $\theta_3 = \theta_4 = -\pi$. Let the power division ratio from port 1 to ports A and B be $1 : k^2$. Using Eq. (4), α and k are related as: $\alpha = \frac{1}{\sqrt{1+k^2}}$.

Based on the mathematical transformations given in [18, 20], mixed-mode scattering matrix is converted into standard scattering matrix. The standard scattering matrix for the proposed five port

UTB PD is given in Eq. (5).

$$[S] = \begin{bmatrix} 0 & -j\frac{\alpha}{\sqrt{2}} & j\frac{\alpha}{\sqrt{2}} & j\frac{\sqrt{1-\alpha^2}}{\sqrt{2}} & -j\frac{\sqrt{1-\alpha^2}}{\sqrt{2}} \\ -j\frac{\alpha}{\sqrt{2}} & -\frac{1}{2} & -\frac{1}{2} & 0 & 0 \\ j\frac{\alpha}{\sqrt{2}} & -\frac{1}{2} & -\frac{1}{2} & 0 & 0 \\ j\frac{\sqrt{1-\alpha^2}}{\sqrt{2}} & 0 & 0 & -\frac{1}{2} & -\frac{1}{2} \\ -j\frac{\sqrt{1-\alpha^2}}{\sqrt{2}} & 0 & 0 & -\frac{1}{2} & -\frac{1}{2} \end{bmatrix} \tag{5}$$

2.3. Analysis of Power Transmission from Input Port to Output Ports

Under the ideal condition, power should flow from input port to two output ports, and no current should flow into two isolation resistors. Equivalent circuit of the proposed PD under this condition is shown in Fig. 3. When no current flows to the isolation resistors, ground point moves to other ends of the resistors. This means that one end of the pair of transmission lines of characteristic impedances Z_3 and Z_4 is connected to the ground. Then other ends of the transmission lines of characteristic impedances Z_3 and Z_4 become open circuited (using the property of quarter-wave transformer).

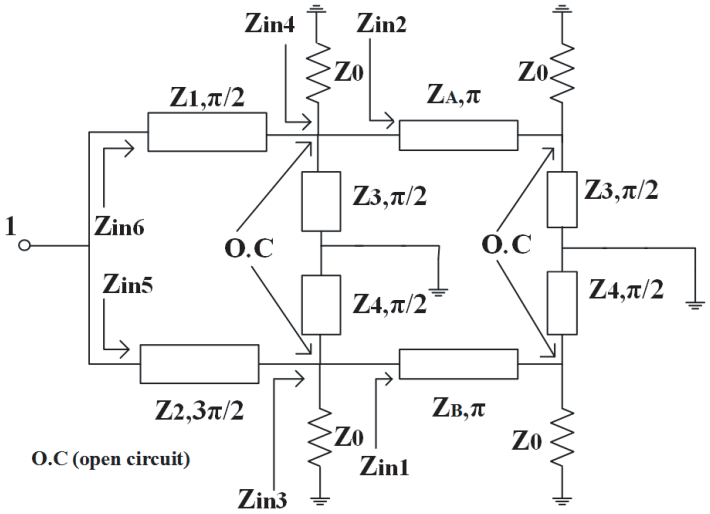

Figure 3. Equivalent circuit for power transmission from input port to output ports.

From Fig. 3, Z_{in1} and Z_{in2} are obtained and given as:

$$Z_{in1} = Z_{in2} = Z_0 \tag{6}$$

Z_{in3} is the parallel combination of Z_0 and Z_{in1} while Z_{in4} is the parallel combination of Z_0 and Z_{in2}. From Fig. 3, Z_{in3} and Z_{in4} are given as:

$$Z_{in3} = Z_{in4} = Z_0/2 \tag{7}$$

Z_{in5} and Z_{in6} are obtained using property of quarter-wave transformer from Fig. 3 and given as:

$$Z_{in5} = \frac{2Z_2^2}{Z_0} \tag{8}$$

$$Z_{in6} = \frac{2Z_1^2}{Z_0} \tag{9}$$

If the power division ratio from port 1 to ports A and B is $1 : k^2$, then Z_{in5} and Z_{in6} are related as:

$$Z_{in6} = k^2 Z_{in5} \tag{10}$$

Using Eqs. (8)–(10), Z_1 and Z_2 are related as:

$$Z_1 = kZ_2 \tag{11}$$

Parallel combination of Z_{in5} and Z_{in6} is equal to Z_0 (port impedance of port 1).

$$Z_{in5} \| Z_{in6} = Z_0 \tag{12}$$

Using Eqs. (8), (9), (11) and (12), Z_1 and Z_2 are derived and given in Eqs. (13) and (14).

$$Z_1 = Z_0 \sqrt{\frac{1+k^2}{2}} \tag{13}$$

$$Z_2 = \frac{Z_0}{k} \sqrt{\frac{1+k^2}{2}} \tag{14}$$

2.4. Isolation Analysis between Two Output Ports

Figure 4 shows the equivalent circuit of proposed PD for this analysis. When port A is exited, no power should flow to port B. It means that voltage and current flowing to port 4 and port 5 (combined as port B) are zero. Therefore, one end of transmission lines of characteristic impedance Z_4 and transmission line of characteristic impedance Z_2 are connected to ground. Then using quarter-wave transformer property, other ends of these transmission lines are open circuited.

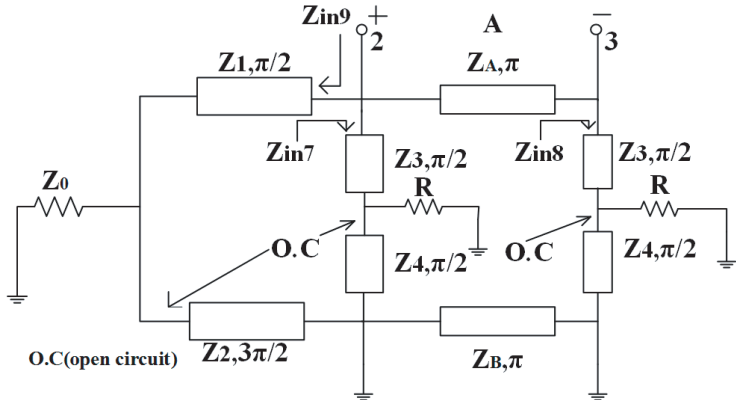

Figure 4. Equivalent circuit for isolation analysis between two output ports.

From Fig. 4, using quarter-wave transformer property, Z_{in7}, Z_{in8} and Z_{in9} are obtained and given as:

$$Z_{in7} = Z_{in8} = \frac{Z_3^2}{R} \tag{15}$$

$$Z_{in9} = \frac{Z_1^2}{Z_0} \tag{16}$$

Let Z_{in10} be the parallel combination of Z_{in7} and Z_{in9}. Using Eqs. (15) and (16), Z_{in10} is obtained and given as:

$$Z_{in10} = Z_{in7} || Z_{in9} = \frac{Z_1^2 Z_3^2}{R Z_1^2 + Z_0 Z_3^2} \tag{17}$$

Transmission parameters matrix between ports 2 & 3 ($[ABCD]_{23}$) is obtained as:

$$\begin{bmatrix} A & B \\ C & D \end{bmatrix}_{23} = \begin{bmatrix} 1 & 0 \\ \dfrac{Z_0}{Z_1^2} + \dfrac{R}{Z_3^2} & 1 \end{bmatrix} \begin{bmatrix} -1 & 0 \\ 0 & -1 \end{bmatrix} \begin{bmatrix} 1 & 0 \\ \dfrac{R}{Z_3^2} & 1 \end{bmatrix} \tag{18}$$

$$\begin{bmatrix} A & B \\ C & D \end{bmatrix}_{23} = \begin{bmatrix} -1 & 0 \\ -\dfrac{Z_0}{Z_1^2} - \dfrac{2R}{Z_3^2} & -1 \end{bmatrix} \tag{19}$$

Scattering matrix between ports 2 & 3 ($[S]_{23}$) can be obtained by matrix conversion from $[ABCD]_{23}$. The elements of matrix $[S]_{23}$ are derived and given in Eqs. (20) and (21).

$$S_{22} = S_{33} = -\frac{Z_0^2 Z_3^2 + 2RZ_0 Z_1^2}{2Z_1^2 Z_3^2 + Z_0^2 Z_3^2 + 2RZ_0 Z_1^2} \tag{20}$$

$$S_{23} = S_{32} = -\frac{2Z_1^2 Z_3^2}{2Z_1^2 Z_3^2 + Z_0^2 Z_3^2 + 2RZ_0 Z_1^2} \tag{21}$$

For port A (combination of ports 2 & 3) to be matched, differential reflection coefficient (S_{ddAA}) of port A should be zero.

$$S_{ddAA} = \frac{1}{2}(S_{22} - S_{23} - S_{32} + S_{33}) = 0 \tag{22}$$

Using Eqs. (20)–(22) and if R is assumed as Z_0, Z_3 is derived and given in Eq. (23).

$$Z_3 = \sqrt{\frac{2Z_1^2}{(2Z_1^2/Z_0^2) - 1}} \tag{23}$$

Similarly, if port B is excited, then no power should flow to port A. After the same process, Z_4 is derived and given in Eq. (24).

$$Z_4 = \sqrt{\frac{2Z_2^2}{(2Z_2^2/Z_0^2) - 1}} \tag{24}$$

2.5. Design Examples

UTB PDs for different power division ratios can be designed using design equations given in Eqs. (13), (14), (23) and (24). For different power division ratios, design parameters are listed in Table 1. It can be noted that Z_A and Z_B are independent parameters and can be chosen independently. While deriving design equations, isolation resistor R is assumed as Z_0 (port impedance) because of the availability of chip resistor. According to the choice of isolation resistor R, design equations can be changed. There is no effect on performance of PD because of the choice of isolation resistor.

Table 1. Design parameters for different power division ratios.

k^2	Z_1	Z_2	Z_3	Z_4
1	50 Ω	50 Ω	70.71 Ω	70.71 Ω
2	61.23 Ω	43.30 Ω	61.23 Ω	86.88 Ω
3	70.71 Ω	40.82 Ω	57.73 Ω	100.03 Ω
4	79.05 Ω	39.52 Ω	55.89 Ω	112 Ω
5	86.60 Ω	38.72 Ω	54.77 Ω	122.75 Ω

Variation of phase difference ($Ang(S_{sd1A}/S_{sd1B})$) and differential-mode power division (S_{sd1A} and S_{sd1B}) with power division ratio are shown in Figs. 5(a) and 5(b), respectively. The results in Fig. 5(a) show that increase in power division ratio leads to increase in deviation from in-phase characteristic. As shown in Fig. 5(b), if power division ratio is unity, differential-mode power is divided equally from unbalanced port to balanced ports. For power division ratios $k^2 = 2$ and $k^2 = 3$, the difference between differential-mode power divisions is 3 dB and 4.77 dB, respectively.

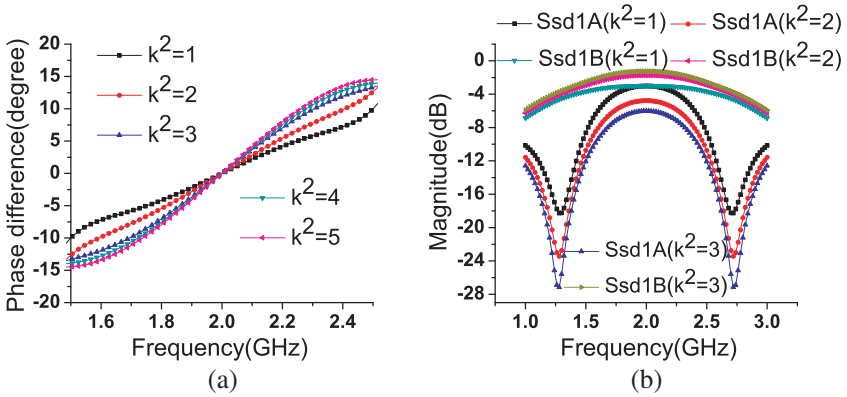

Figure 5. (a) Variation of phase difference with power division ratio. (b) Differential-mode power division to balanced ports for different values of power division ratio.

3. RESULTS AND DISCUSSIONS

3.1. Comparison of Theoretical and Simulation Results

The proposed UTB PD with arbitrary power division is designed at 2 GHz. Power division ratio (k^2) is taken as 2. Isolation resistor R is taken as 50 Ω. Design parameters for $k^2 = 2$ are taken from Table 1. Z_A and Z_B are taken the same as Z_1 and Z_2, respectively. A circuit model is designed using the circuit parameters obtained at design frequency. The electrical lengths of the transmission line sections used in the design vary with frequency which changes the response of the circuit. Complete theoretical responses are obtained by applying frequency sweep in the circuit model. For theoretical results, lossless transmission lines and ideal lumped components are used.

Planar microstrip technology is used to realize the proposed UTB PD. The proposed PD is designed on an FR-4 substrate of dielectric constant $\epsilon_r = 4.4$ and thickness $h = 1.6$ mm. For very thin conductors, close-form expressions for design in microstrip technology are reported in [21]. These relations are summarized as:

For $W/h \leq 1$:

$$\epsilon_{re} = \frac{\epsilon_r + 1}{2} + \frac{\epsilon_r - 1}{2}\left[\left(1 + 12\frac{h}{W}\right)^{-0.5} + 0.04\left(1 - \frac{W}{h}\right)^2\right] \tag{25}$$

$$Z_c = \frac{\eta}{2\pi\sqrt{\epsilon_{re}}} \ln\left(\frac{8h}{W} + 0.25\frac{W}{h}\right) \tag{26}$$

For $W/h \geq 1$:

$$\epsilon_{re} = \frac{\epsilon_r + 1}{2} + \frac{\epsilon_r - 1}{2}\left(1 + 12\frac{h}{W}\right)^{-0.5} \tag{27}$$

$$Z_c = \frac{\eta}{\sqrt{\epsilon_{re}}}\left[\frac{W}{h} + 1.393 + 0.677\ln\left(\frac{W}{h} + 1.444\right)\right]^{-1} \tag{28}$$

where ϵ_{re}, ϵ_r, h, W, Z_c and η are effective dielectric constant, dielectric constant of substrate, thickness of the substrate, width of the transmission line, characteristic impedance of the transmission line and wave impedance in free space, respectively.

Relation between electrical length θ and physical length L is also reported in [21] and summarized as:

$$\theta = \beta L = \frac{2\pi}{\lambda_g} L \tag{29}$$

$$\lambda_g = \frac{\lambda_0}{\sqrt{\epsilon_{re}}},\ \lambda_0 = \frac{c}{f} \tag{30}$$

where λ_g, λ_0, c and f are guided-wavelength, free space wavelength, velocity of light and operating frequency, respectively.

Based on Eqs. (25)–(30), structure of the proposed PD is designed with microstrip technology. The structure is simulated and optimized using HFSS. Comparisons of theoretical and simulated results are shown in Figs. 6–8(a).

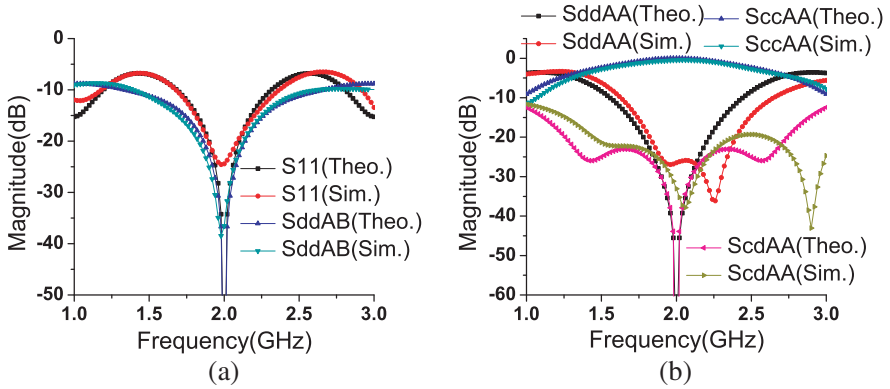

Figure 6. (a) Comparison of theoretical and simulation results of $|S_{ss11}|$ and $|S_{ddAB}|$. (b) Comparison of theoretical and simulation results of $|S_{ddAA}|$, $|S_{ccAA}|$ and $|S_{cdAA}|$.

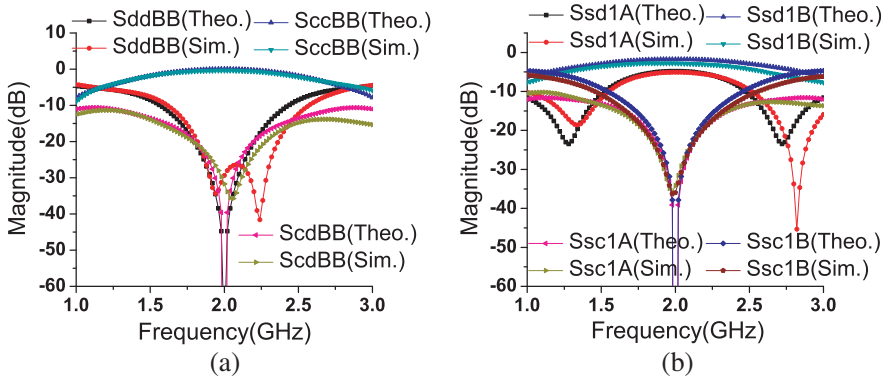

Figure 7. (a) Comparison of theoretical and simulation results of $|S_{ddBB}|$, $|S_{ccBB}|$ and $|S_{cdBB}|$. (b) Comparison of theoretical and simulation results of $|S_{sd1A}|$, $|S_{sd1B}|$, $|S_{sc1A}|$ and $|S_{sc1B}|$.

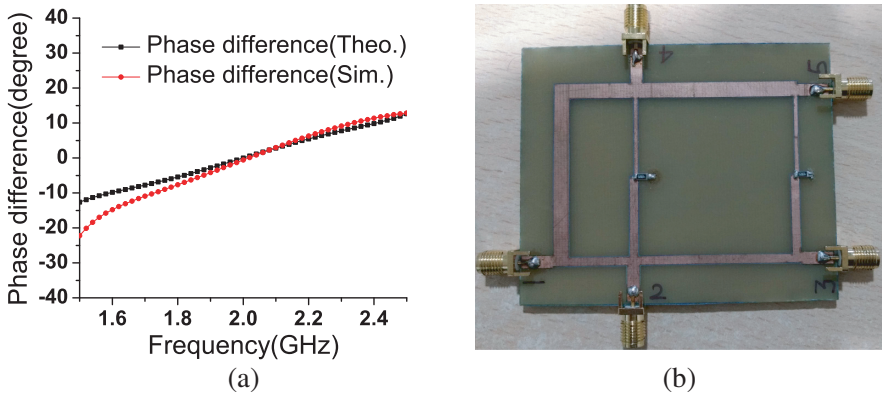

Figure 8. (a) Comparison of theoretical and simulation results of phase difference. (b) Fabricated prototype of proposed PD for $k^2 = 2$.

In Fig. 6(a), theoretical and simulated results of $|S_{11}|$ show that input port is perfectly matched at design frequency. Theoretical and simulated results of $|S_{ddAB}|$ in Fig. 6(a) show that balanced ports are perfectly isolated at design frequency. Theoretical and simulated results of $|S_{ddAA}|$, $|S_{ccAA}|$ and $|S_{cdAA}|$ are shown in Fig. 6(b), and results of $|S_{ddBB}|$, $|S_{ccBB}|$ and $|S_{cdBB}|$ are shown in Fig. 7(a). These results show that balanced ports A & B are perfectly matche, that common-mode reflections of both ports are close to 0 dB, and that no conversion between differential and common-mode at ports A & B. Theoretical and simulated results of $|S_{sd1A}|$, $|S_{sd1B}|$, $|S_{sc1A}|$ and $|S_{sc1B}|$ are shown in Fig. 7(b). Theoretical results of $|S_{sd1A}|$ and $|S_{sd1B}|$ are -4.7 dB, -1.7 dB at design frequency. It shows that the difference between differential-mode power divisions in port A and port B is 3 dB. Results of $|S_{sc1A}|$ and $|S_{sc1B}|$ show that common-modes are perfectly suppressed from unbalanced port to balanced ports. Fig. 8(a) shows theoretical and simulated results of phase difference. It shows in-phase characteristic of PD around design frequency.

The theoretical and simulated fractional bandwidths are 27% (from 1.72 GHz to 2.26 GHz) and 23% (from 1.80 GHz to 2.26 GHz), respectively. The conditions for calculating the fractional bandwidth are: (i) Difference between $|S_{sd1B}|$ and $|S_{sd1A}|$ is less than 4 dB; (ii) $|S_{ccAA}|$ and $|S_{ccBB}|$ are less than 1 dB; (iii) All other scattering parameters are greater than 10 dB.

3.2. Comparison of Simulation and Measured Results

The prototype of proposed UTB PD is fabricated for power division ratio $k^2 = 2$ and shown in Fig. 8(b). Fig. 9(a) shows the layout of fabricated prototype. All dimensions shown in Fig. 9(a) are listed in Table 2. Measurement is done using two-port VNA (vector network analyzer). Single-ended scattering parameters are measured directly from VNA while mixed-mode scattering parameters are obtained using mathematical transformations described in [18, 20]. Figs. 9(b)–11 show the comparison of simulated and measured results.

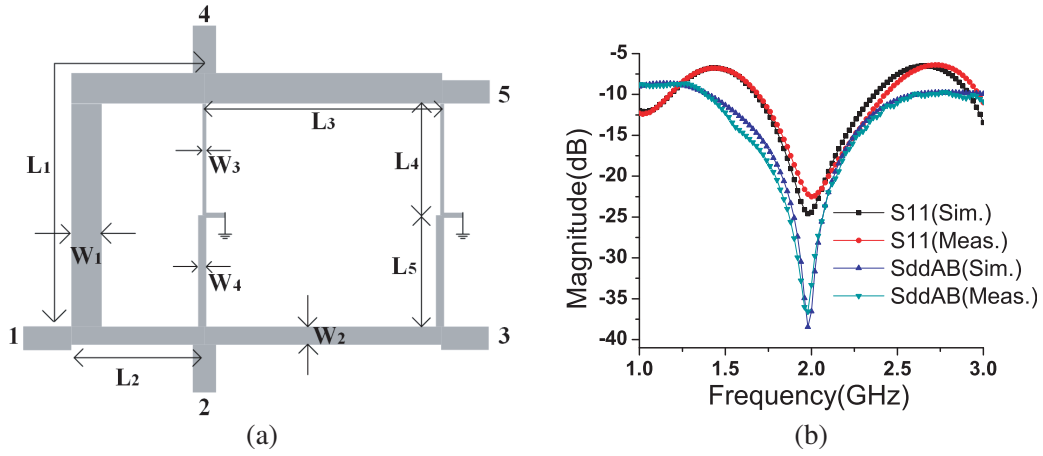

Figure 9. (a) Layout of the fabricated prototype of proposed PD for $k^2 = 2$. (b) Comparison of $|S_{ss11}|$ and $|S_{ddAB}|$.

Table 2. Layout dimensions of fabricated prototype.

W_1	W_2	W_3	W_4	L_1	L_2	L_3	L_4	L_5
3.81 mm	2.09 mm	0.97 mm	2.09 mm	63.1 mm	20.5 mm	38.4 mm	21 mm	21 mm

Figure 9(b) shows the comparison of simulated and measured return losses of single-ended input port ($|S_{ss11}|$) and isolation ($|S_{ddAB}|$) between two balanced output ports. Measured $|S_{ss11}|$ is greater than 15 dB from 1.84 GHz to 2.24 GHz, and measured $|S_{ddAB}|$ is greater than 20 dB from 1.80 GHz to 2.14 GHz (fractional bandwidth of 17%). Fig. 10(a) shows common-mode reflection ($|S_{ccAA}|$),

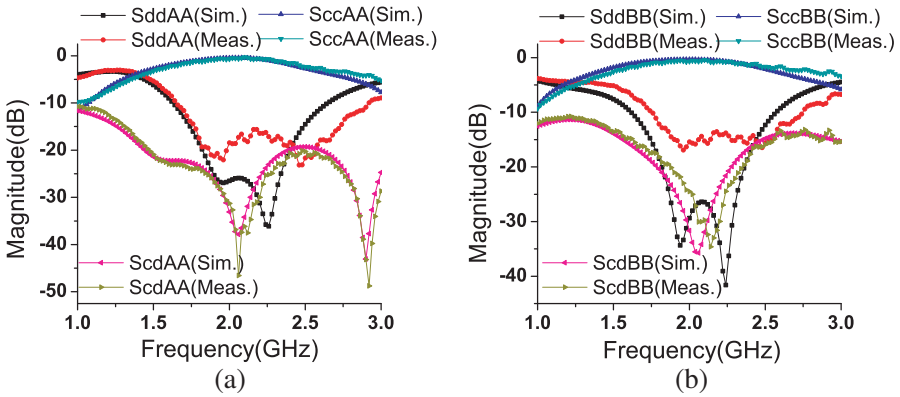

Figure 10. (a) $|S_{ddAA}|$, $|S_{ccAA}|$ and $|S_{cdAA}|$. (b) Comparison of $|S_{ddBB}|$, $|S_{ccBB}|$ and $|S_{cdBB}|$.

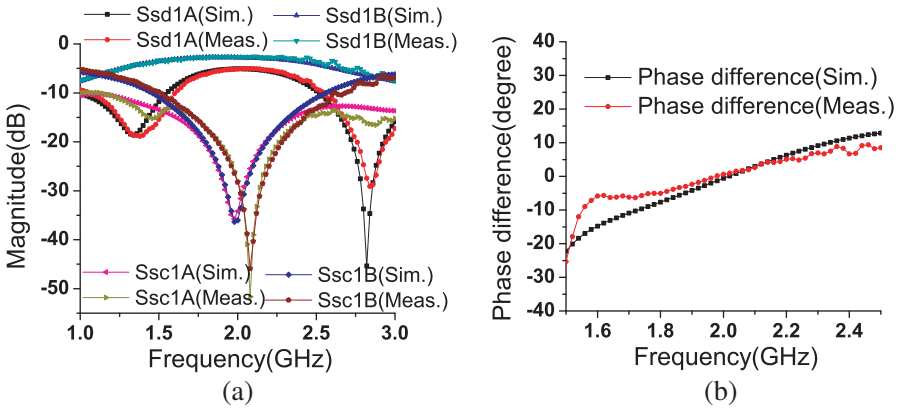

Figure 11. (a) Comparison of $|S_{sd1A}|$, $|S_{sd1B}|$, $|S_{sc1A}|$ and $|S_{sc1B}|$. (b) Comparison of phase difference.

differential-mode return loss ($|S_{ddAA}|$), differential to common-mode conversion ($|S_{cdAA}|$) of the balanced port A, respectively. Measured $|S_{ccAA}|$ is less than 1 dB from 1.86 GHz to 2.28 GHz. Measured $|S_{ddAA}|$ is greater than 15 dB from 1.78 GHz to 2.72 GHz. Measured $|S_{cdAA}|$ is greater than 25 dB from 1.86 GHz to 2.26 GHz. Fig. 10(b) shows common-mode reflection ($|S_{ccBB}|$), differential-mode return loss ($|S_{ddBB}|$), differential to common-mode conversion ($|S_{cdBB}|$) of the balanced port B, respectively. Measured $|S_{ccBB}|$ is less than 1 dB from 1.76 GHz to 2.28 GHz. Measured $|S_{ddBB}|$ is greater than 10 dB from 1.76 GHz to 2.74 GHz. Measured $|S_{cdBB}|$ is greater than 20 dB from 1.88 GHz to 2.34 GHz. The measured $|S_{ddAA}|$ and $|S_{ddBB}|$ show wide-band characteristic compared with their theoretical results. In Fig. 11(a), measured common-mode suppression to balanced ports A and B ($|S_{sc1A}|$ and $|S_{sc1B}|$) is greater than 20 dB from 1.9 GHz to 2.18 GHz. Differential-mode powers ($|S_{sd1A}|$ and $|S_{sd1B}|$) are divided in power division ratio 1 : 2 around design frequency. Fig. 11(b) shows the comparison of simulated and measured phase differences ($Ang(S_{sd1A}/S_{sd1B})$). Measured phase difference is within $\pm 5^\circ$ from 1.8 GHz to 2.2 GHz, and simulated phase difference is within $\pm 5^\circ$ from 1.86 GHz to 2.16 GHz. This shows the in-phase characteristic of proposed PD.

The measured fractional bandwidth is 21% (from 1.86 GHz to 2.28 GHz) based on the conditions mentioned while calculating theoretical and simulated fractional bandwidths.

3.3. Comparison with Previous Related Works

Comparisons with previously related works are summarized in Table 3. The PD reported in [17] is designed using balun, and mixed-mode scattering parameters are not evaluated in the reported paper. Therefore, isolation and CMS characteristic are not provided. In [17], fractional bandwidth is evaluated only by considering return loss of input port. The PDs reported in [19, 20] are of Wilkinson type. In

Table 3. Comparison with previous related works.

Ref.	Freq. (GHz)	Type	Isolation (dB)	CMS (dB)	Bandwidth	Transmission Loss (dB)
[17]	5	Equal	NA	NA	80% (RL)	0.5
[19]	1.8	Equal	> 20	> 20	17%(Isolation)	0.15
[20]	1	Equal	> 20	> 20	37%	0.34
This work	2	Arbitrary $(1 : 2)$	> 20	> 20	21%	0.56

CMS: Common-mode suppression, NA: Not available, RL: Return loss

general, transmission loss of a Wilkinson PD is better than a Gysel PD. Therefore, the PDs reported in [19, 20] have better performance in terms of transmission loss. In [19], bandwidth for each scattering parameter is reported separately, and isolation bandwidth is listed in the comparison table which is equal to isolation bandwidth of this work. All the previous reported UTB PDs presented in comparison table are designed for equal power division.

In the present work, a UTB PD for arbitrary power division is presented, and a PD for $k^2 = 2$ is fabricated and tested. Isolation and CMS results of this work are similar to the previous reported works. Fractional bandwidth of this work is 21% which is calculated by considering all scattering parameters. Transmission loss at the design frequency is 0.56 dB.

4. CONCLUSION

A Gysel type UTB PD with arbitrary power division is presented in this paper. Design equations are derived analytically. Using design equations, UTB PDs can be designed for different power division ratios. For different power division ratios ($k^2 = 1$ to $k^2 = 5$), design parameters are listed in this paper. UTB PD for equal power division is a special case of this proposed work. A UTB PD is designed for $1 : 2$ power division ratio, and performance of the device is evaluated using HFSS. A prototype is also fabricated and tested. Measured results agree with simulated ones, and the analytically obtained design equations are thus validated. Measured fractional bandwidth of fabricated circuit is 21%. Greater than 20 dB isolation between balanced ports is achieved. In-phase characteristic of fabricated circuit is within $\pm 5^\circ$. The proposed configuration is of Gysel type; therefore, this configuration can also be useful for high power applications.

REFERENCES

1. Xia, B., L. S. Wu, and J. Mao, "A new balanced-to-balanced power divider/combiner," *IEEE Transactions on Microwave Theory and Techniques*, Vol. 60, 2791–2798, Sept. 2012.
2. Xia, B., L. S. Wu, S. W. Ren, and J. F. Mao, "A balanced-to-balanced power divider with arbitrary power division," *IEEE Transactions on Microwave Theory and Techniques*, Vol. 61, 2831–2840, Aug. 2013.
3. Wu, L. S., Y. X. Guo, and J. F. Mao, "Balanced-to-balanced gysel power divider with bandpass filtering response," *IEEE Transactions on Microwave Theory and Techniques*, Vol. 61, 4052–4062, Dec. 2013.
4. Wilkinson, E. J., "An n-way hybrid power divider," *IRE Transactions on Microwave Theory and Techniques*, Vol. 8, 116–118, Jan. 1960.
5. Gysel, U. H., "A new n-way power divider/combiner suitable for high-power applications," *1975 IEEE-MTT-S International Microwave Symposium*, 116–118, May 1975.
6. Wang, K. X., X. Y. Zhang, and B. J. Hu, "Gysel power divider with arbitrary power ratios and filtering responses using coupling structure," *IEEE Transactions on Microwave Theory and Techniques*, Vol. 62, 431–440, Mar. 2014.

7. Sun, Z., L. Zhang, Y. Yan, and H. Yang, "Design of unequal dual-band gysel power divider with arbitrary termination resistance," *IEEE Transactions on Microwave Theory and Techniques*, Vol. 59, 1955–1962, Aug. 2011.
8. Du, Y. L. M., H. Peng, and W. Zhou, "A miniaturized gysel power divider/combiner using planar artificial transmission line," *Progress In Electromagnetics Research C*, Vol. 51, 79–86, 2014.
9. Fartookzadeh, S. H. M. A. M. and M. Kazerooni, "A novel 180° hybrid based on the modified gysel power divider," *Progress In Electromagnetics Research C*, Vol. 27, 209–222, 2012.
10. Shahi, H. and H. Shamsi, "Compact wideband gysel power dividers with harmonic suppression and arbitrary power division ratios," *AEU — International Journal of Electronics and Communications*, Vol. 79, 16–25, 2017.
11. Wang, X., K. L. Wu, and W. Y. Yin, "A compact gysel power divider with unequal power-dividing ratio using one resistor," *IEEE Transactions on Microwave Theory and Techniques*, Vol. 62, 1480–1486, Jul. 2014.
12. Chen, S., T. Zhang, T. Huang, and Y. Yu, "A planar out-of-phase power divider with unequal power dividing ratio," *Progress In Electromagnetics Research Letters*, Vol. 63, 37–43, 2016.
13. Xu, K., J. Shi, L. Lin, and J. X. Chen, "A balanced-to-unbalanced microstrip power divider with filtering function," *IEEE Transactions on Microwave Theory and Techniques*, Vol. 63, 2561–2569, Aug. 2015.
14. Zhang, W., Y. Wu, Y. Liu, F. M. Ghannouchi, and A. Hasan, "A wideband balanced-to-unbalanced coupled-line power divider," *IEEE Microwave and Wireless Components Letters*, Vol. 26, 410–412, Jun. 2016.
15. Yadav, A. N. and R. Bhattacharjee, "Balanced to unbalanced out of phase equal power divider for wide-band application," *2016 Asia-Pacific Microwave Conference (APMC)*, 1–4, Dec. 2016.
16. Yadav, A. N. and R. Bhattacharjee, "Balanced to unbalanced power divider with arbitrary power ratio," *IEEE Microwave and Wireless Components Letters*, Vol. 26, 885–887, Nov. 2016.
17. Muralidharan, S., K. Wu, and M. Hella, "A compact low loss single-ended to two-way differential power divider/combiner," *IEEE Microwave and Wireless Components Letters*, Vol. 25, 103–105, Feb. 2015.
18. Yu, Y. and L. Sun, "A design of single-ended to differential-ended power divider for x band application," *Microwave and Optical Technology Letters*, Vol. 57, No. 11, 2669–2673, 2015.
19. Shi, J., K. Xu, W. Zhang, J. X. Chen, and G. Zhai, "An approach to 1-to-2n way microstrip balanced power divider," *IEEE Transactions on Microwave Theory and Techniques*, Vol. 64, 4222–4231, Dec. 2016.
20. Zhang, W., Y. Liu, Y. Wu, A. Hasan, F. M. Ghannouchi, Y. Zhao, X. Du, and W. Chen, "Novel planar compact coupled-line single-ended-to-balanced power divider," *IEEE Transactions on Microwave Theory and Techniques*, Vol. PP, No. 99, 1–11, 2017.
21. Hong, J.-S. and M. J. Lancaster, *Microstrip Filters for RF/Microwave Applications*, John Wiley & Sons, Inc., New York, 2001.